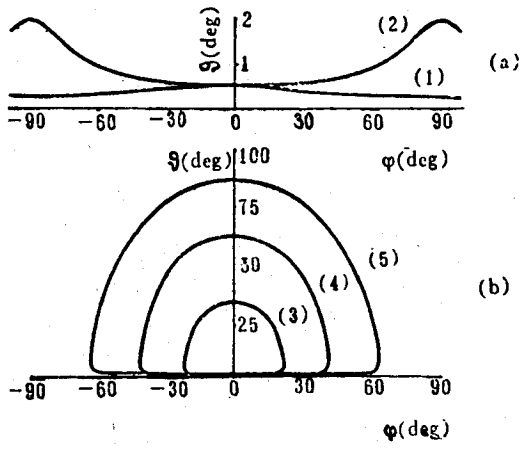

Fig. 3 Trajectories in $\varphi - \vartheta$ plane.

despun-motor torque, the kinetic energy is conservative.

$$T = (\tfrac{1}{2})\,\omega \cdot I \cdot \omega + \Omega \cdot B \cdot \omega + (\tfrac{1}{2})\,\Omega \cdot B \cdot \Omega = \text{const} \qquad (18)$$

So, besides H and Γ, another first integral σ can be expressed as

$$\sigma = (2T - B_1\Gamma^2)/I_3\nu^2 = (A_1\omega_1^2 + I_2\omega_2^2 + I_3\omega_3^2)/I_3\nu^2 \qquad (19)$$

Putting Eq. (10) into the above equation and letting $\Gamma/\nu = k$, one arrives at

$$\sigma = (\lambda c\vartheta - \mu k)^2/\lambda + s^2\vartheta[1 + (\rho - 1)s^2\varphi] \qquad (20)$$

The integral σ can be determined in terms of the initial values ϑ_0, φ_0, Γ_0, and ω_{10}. The system parameters for a dual-spin spacecraft example are as follows:

$$I_1 = 480 \text{ kgm}^2 \quad I_2 = 360 \text{ kgm}^2$$

$$I_3 = 440 \text{ kgm}^2 \quad B_1 = 160 \text{ kgm}^2$$

$$\vartheta_0 = 0.5 \text{ deg} \quad \varphi_0 = 0 \quad \Gamma_0 = 1.0 \text{ rad/s}$$

1) $\omega_{10} = 1.0$ rad/s
2) $\omega_{10} = 4.5$ rad/s
} stable cases

3) $\omega_{10} = 1.5$ rad/s
4) $\omega_{10} = 2.0$ rad/s
5) $\omega_{10} = 3.0$ rad/s
} unstable cases (21)

The above parameters, except ϑ_0, are the same as those in Ref. 4, from which one can draw trajectories in $\varphi - \vartheta$ plane by using Eq. (20) (see Fig. 3).

Figure 3 shows that if the initial values of nutational angle ϑ_0 are small, then ϑ will change in the small angular region for stable cases and will change into larger values for unstable cases. The nutational angle ϑ and spin angle φ in Fig. 3 have more obvious physical meanings than R and θ in Fig. 2 of Ref. 4. By comparing, one can see that the trajectory (5) in Fig. 2 of Ref. 4 is not correct. The reason is that it is not correct to replace I_{A3} by I to obtain Eq. (24) from Eq. (14b).

Conclusion

A new method for the nutational stability analysis of an asymmetric dual-spin spacecraft is presented. It is directly derived from the first-order differential equations of the system. The behavior of nutational motion is investigated with the aid of the energy integral of the system. The method can also be expanded to discuss nutational stability of a dual-spin spacecraft composed of two asymmetric bodies.

References

[1]Leimanis, E., *The General Problem of the Motion of Coupled Rigid Bodies About a Fixed Point,* Springer-Verlag, New York, 1965, pp. 207–232.

[2]Kane, T.R., "Solution of the Equations of Rotational Motion for a Class of Torque-Free Gyrostats," *AIAA Journal,* Vol. 8, June 1970, pp. 1141–1143.

[3]Cochran, J.E., Shu, P.H., and Rew, S.D., "Attitude Motion of Asymmetric Dual-Spin Spacecraft," *Journal of Guidance, Control, and Dynamics,* Vol. 5, Jan.-Feb. 1982, pp. 37–42.

[4]Tsuchiya, K., "Attitude Behavior of a Dual-Spin Spacecraft Composed of Asymmetric Bodies," *Journal of Guidance and Control,* Vol. 2, July-Aug. 1979, pp. 328–333.

[5]Liu, Y.Z., "A New Approach to the Motion of Rigid Body About a Fixed Point in Euler's Case," *Journal of Shanghai Mechanics,* Vol. 2, No. 3, 1981, pp. 52–55.

Sensor Failure Detection Using Generalized Parity Relations for Flexible Structures

Mathieu Mercadal*
Massachusetts Institute of Technology, Cambridge, Massachusetts

I. Introduction

GENERALIZED single-sensor parity relations (GSSPR) are an attractive method of fault detection and isolation (FDI) for large-scale systems such as space structures with a potentially great number of sensors.[1] GSSPR belongs, indeed, to the class of analytical redundancy methods that alleviate the need for replicating hardware components. Instead, a failure is indicated by the occurrence of a mismatch between the history of the actual sensor outputs and the history predicted using the analytical model.[2] GSSPR also leads to very simple isolation logic. Finally, generating the relations is particularly easy when the eigenstructure of the system is known, which is usually the case for flexible structures whose modeling is obtained via finite-element analysis. The method, unfortunately, suffers many shortcomings, one of which is a high sensitivity to modeling error and noise, as demonstrated in this paper by GSSPR test results obtained on the NASA Langley Spacecraft Control Laboratory Experiment (SCOLE). Part II of this paper treats GSSPR generation. Test results are presented in part III. Part IV concludes the paper.

II. Generalized Single-Sensor Parity Relations

Consider a discrete-time lumped parameter model describing the dynamics of a structure:

$$X(i+1) = A\,X(i) + B\,U(i) \qquad (1)$$

where $X(i)$ is the state vector at time i, $U(i)$ contains all the command inputs, A and B are two constant coefficient matrices. A standard way to obtain such a model is through finite-element analysis.[3] Such a technique directly yields the continuous model in modal form. The discretization is a standard procedure.[4]

Received Oct. 8, 1987; revision received Jan. 26, 1988.

*Graduate Student, Research Assistant.

The measurement equation for any sensor has the form

$$y(i) = \boldsymbol{C}\, X(i) + \boldsymbol{D}\, U(i) \tag{2}$$

where $\boldsymbol{C}$ and $\boldsymbol{D}$ are row vectors. The vector sequence of measurements $\mathcal{Y}(i) = [y(i), y(i+1), \cdots y(i+N)]^T$ can be related to the state vector at the instant i and the input sequence vector $\mathcal{U}(i) = [U(i)^T, U(i+1)^T, \cdots U(i+N)^T]^T$ in a linear way as follows:

$$\mathcal{Y}(i) = \begin{bmatrix} \boldsymbol{C}\boldsymbol{I} \\ \boldsymbol{C}\boldsymbol{A} \\ \vdots \\ \boldsymbol{C}\boldsymbol{A}^N \end{bmatrix} X(i) + \begin{bmatrix} \boldsymbol{D} & 0 & \cdots & 0 \\ \boldsymbol{C}\boldsymbol{B} & \boldsymbol{D} & & 0 \\ \vdots & \vdots & & \vdots \\ \boldsymbol{C}\boldsymbol{A}^{N-1}\boldsymbol{B} & \boldsymbol{C}\boldsymbol{A}^{N-2}\boldsymbol{B} \cdots & \boldsymbol{C}\boldsymbol{B} & \boldsymbol{D} \end{bmatrix} \mathcal{U}(i) \tag{3}$$

or, in short:

$$\mathcal{Y}(i) = \boldsymbol{C}^*\, X(i) + \beta\, \mathcal{U}(i) \tag{4}$$

As N increases, more rows are added to $\boldsymbol{C}^*$, which will eventually have a left null-space. For such an N, there exists a normalized row vector $\boldsymbol{W}$ such that $\boldsymbol{W}\,\boldsymbol{C}^* = 0$. In that case, and when the system is conformed to its model (no-fail mode), the quantity

$$r(i) = \boldsymbol{W}[\mathcal{Y}(i) - \beta\, \mathcal{U}(i)] = \boldsymbol{W}\,\boldsymbol{C}^*\, X(i) \tag{5}$$

should be identically zero, or at least zero-mean; $r(i)$ is the residual for the considered sensor at time $i+N$. If $r(i)$ deviates significantly from zero, then either the measurement Eq. (2) is not satisfied, or some actual input to the plant differs from its command value. Such an occurrence indicates a failure, but note that a single-sensor parity relation is unaffected by failures of sensors other than the one for which it is designed.

If the characteristic polynomial of $\boldsymbol{A}$ is

$$\phi(z) = w_R z^R + w_{R-1} z^{R-1} + \cdots + w_1 z + w_0 \tag{6}$$

then, by the Cayley-Hamilton theorem

$$[w_0\ w_1 \cdots w_R]\ \boldsymbol{C}^* = \boldsymbol{C} \cdot \{w_R \boldsymbol{A}^R + w_{R-1}\boldsymbol{A}^{R-1} + \cdots + w_1 \boldsymbol{A} + w_0 \boldsymbol{I}\} = 0 \tag{7}$$

Parity vectors are thus closely related to the poles of the system. A recent result[5] shows that to get the parity vector of smallest length, one only needs 1) to consider the modes that are observable from the particular sensor of interest, and 2) to compute the coefficients of the polynomial whose roots are those observable modes, taken with multiplicity 1. Regrouping the coefficients of the polynomial in ascending order yields the desired $\boldsymbol{W}$ vector. This polynomial is for a flexible structure

$$\varphi(z) = \Pi\{z^2 - 2\cos(\sqrt{1-\zeta_i^2}\,\omega_i \Delta t) \cdot \exp(-\zeta_i \omega_i \Delta t) \cdot z + \exp(-2\zeta_i \omega_i \Delta t)\}\ i \in \Omega \tag{8}$$

where Δt is the sampling period, Ω is the set of the indices of the modes observable by the sensor of interest, ω_i and ζ_i are the frequency and the damping ratio of the ith mode. The simplicity of the method to generate parity relations makes the computation fast, efficient, and free of numerical problems. As the eigenmodel of the structure is always available, such a technique is particularly attractive.

III. Evaluation of GSSPR on the SCOLE

The NASA Langley SCOLE[6] reproduces many of the features of a flexible satellite. It is made of a massive plate under which is suspended a long slender mast that carries at its other end an hexagonally shaped structure representing an antenna reflector. The plate hangs from the roof attached to a long cable at the system's center of mass. The plate can also be clamped to perform experiments on the flexible part only. The system is instrumented with a variety of sensors and actuators.

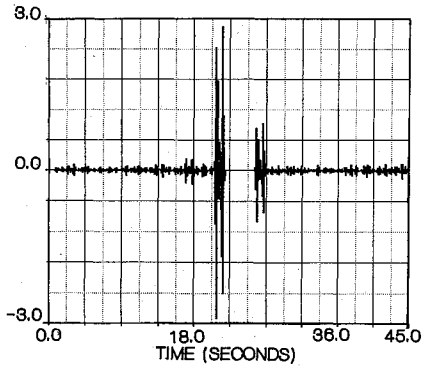

Fig. 1 Residual history for plate-mounted accelerometer.

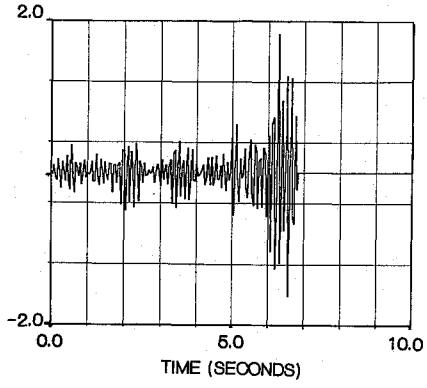

Fig. 2 Residual history for reflector-mounted accelerometer.

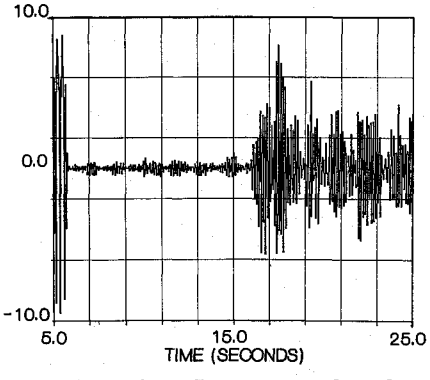

Fig. 3 Residual history for reflector-mounted accelerometer in the presence of thruster activity.

GSSPR generated as shown in part II were tested for various sensors. Up to 10 modes were kept in the model. Figure 1 shows the residual history for one accelerometer located on the heavy plate. The plot was generated off-line using the data of a minimum time slew maneuver performed with the plate free. The actuators used were two cold gas jets located at the tip of the mast on the reflector structure. The measurement was forced to zero between $t = 20$ and $t = 25$ s to simulate a failure. Figures 2 and 3 show the residual histories for an accelerometer located on the reflector structure at the tip of the flexible mast with the plate clamped. Figure 2 corresponds to the free oscillation of the mast and the reflector. A failure (measurement forced to zero) occurs at $t = 6$ s. Figure 3 corresponds to an experiment with an active

vibration suppression control loop using the cold gas jets located on the reflector.

The main lesson of the tests is that the performance of the method is highly dependent on modeling error: the sensor of interest on Fig. 1 is located on the rigid part of the structure, which is modeled with good accuracy. The signature of the failure is obvious in that case. On Fig. 2, the sensor is located in the flexible part of the structure where a 10% discrepancy was already observed on the period of third mode. The noise due to modeling error largely obscures the failure signature in that case. The most dramatic result appears on Fig. 3 where the first firing of a jet occurs at $t = 16$ s. The failure detectability keeps deteriorating as the model becomes less accurate, and only in case 1 can a failure be really detected. Case 3 includes the large modeling errors of the higher modes that are excited by the jets, as well as the effects of the unmodeled dynamics of the actuators and a variety of subsystems (valves, feedlines) necessary for the functioning of the jets, and some overlooked problems of electrical interferences between the actuator and collocated sensors, which increase the measurement noise.

The tests also illustrate the drawbacks arising from the impossibility to enhance failure detectability. As shown in part II, the characteristics of the parity relations are dictated by the system's dynamics. Using the transfer function terminology, the generalized parity relation must have its zero cancelling the observable poles of the system.[5] An unfortunate consequence of this, which is specific to the SCOLE and to flexible structures, is the small, or zero, steady-state gain of the GSSPR. The SCOLE has an observable pole at zero in the free configuration, and a very low-frequency mode in the clamped configuration. Thus, steady-state biases do not create any bias in the residuals (Figs. 1 and 2). Once the transient has died out, one cannot detect offsets in the measurement.

Conclusion

Analytical redundancy has to be preferred to hardware redundancy to perform FDI on large-scale systems like space structures. GSSPR are an answer to this FDI problem, which offer two main advantages: they lead to a very simple isolation logic, and their generation is extremely fast, even with very complex systems, if the eigenstructure of the system is known. However, GSSPR suffer poor performance: the main problem arising in their implementation is the very high sensitivity of the residuals to modeling error and noise. Very detailed and accurate models must, therefore, be available, or FDI will be impossible. A second drawback of the method is that the failure signature cannot be shaped. In the more specific case of a structure with observable poles at the origin, steady failures like biases do not produce a steady offset of the residuals, but only a transient signature. The implementation of GSSPR will, therefore, necessitate the use of sophisticated detection algorithms to decide on a failure based on the values of the residuals.

Acknowledgment

This work was supported by NASA Langley Research Center under Research Grant NAG 1-126.

References

[1]Dutilloy, J., "Generalized Parity Relations for Large Space Structures with Uncertain Parameters," S. M. Thesis, Dept. of Aeronautics and Astronautics, Massachusetts Inst. of Technology, Feb. 1986.

[2]Chow, E. Y. and Willsky, A. S., "Analytical Redundancy and the Design of Robust Failure Detection Systems," *IEEE Transactions on Automatic Control,* Vol. AC-29, July 1984, pp. 603–614.

[3]Meirovitch, L., *Computational Methods in Structural Dynamics,* Sythoff-Noordhoff, APphen aan der Rijn, the Netherlands, 1980.

[4]Franklin, G. F. and Powell, J. D., *Digital Control of Dynamic Systems,* Addison-Wesley, Reading, MA, 1980, Chap. 6.

[5]Massoumnia, M.-A. and Vander Velde, W. E., "Generating Parity Relations for Detecting and Identifying Control System Component Failures," *Journal of Guidance, Control, and Dynamics,* Vol. 11, Jan.–Feb. 1988, pp. 60–65.

[6]Williams, J. and Rallo, A., "Description of the Spacecraft Control Laboratory Experiment (SCOLE) Facility," NASA TM-89057, Jan. 1987.